



Quantization of electronic states in individual oxide-supported silver particles

Niklas Nilus^{*}, Maria Kulawik, Hans-Peter Rust, Hans-Joachim Freund

Fritz-Haber Institut der MPG, Chemical Physics, Faradayweg 4-6, D14195 Berlin, Germany

Received 15 June 2004; accepted for publication 3 September 2004
Available online 23 September 2004

Abstract

The electronic properties of Ag particles on $\text{Al}_2\text{O}_3/\text{NiAl}(110)$ have been investigated by low-temperature scanning tunnelling microscopy and spectroscopy. Conductance measurements on single clusters revealed a series of equidistant resonances around the Fermi level. The energy separation between these peaks decreases with increasing cluster size. The resonances were interpreted as a discretization of the electronic states along the cluster height. In conductance images of the Ag particles, resonance levels appear as concentric circles of enhanced conductance with a diameter depending on the sample bias. This behaviour reflects the influence of the tip electric field on level positions in the clusters.

© 2004 Elsevier B.V. All rights reserved.

Keywords: Scanning tunneling microscopy; Scanning tunneling spectroscopies; Clusters; Surface electrical transport (surface conductivity, surface recombination, etc.); Silver; Aluminum oxide

Metal particles on non-interacting surfaces have been intensively studied over the last decade, using a variety of surface science techniques. This unbroken fascination results from the specific properties of matter under spatial confinement. The reduction in size induces a breakdown of the bulk band structure. Gaps open between the electronic states, the k dispersion becomes softened and the system

finally breaks into a number of discrete electron levels. This evolution of electronic properties with size is accompanied by dramatic changes in the optical, chemical and magnetic behaviour of small particles with respect to bulk materials [1–3]. Various applications in heterogeneous catalysis and optics are already based on the distinct properties of confined metal systems. Several potential uses stimulate further experimental and theoretical efforts for a detailed characterization.

The investigation of nano-particles is still an experimental challenge. The distinct size dependence

^{*} Corresponding author. Tel.: +493084134191; fax: +493084134101.

E-mail address: nilius@fhi-berlin.mpg.de (N. Nilius).

of their properties causes strong inhomogeneous broadening effects in experiments on cluster ensembles, covering the electronic signature of an individual cluster [4,5]. This problem can be circumvented by the use of local probes, such as scanning tunnelling microscopy (STM). Its unrivalled spatial resolution allows the topographic characterization of single clusters down to the atomic scale [6]. In combination with scanning tunnelling spectroscopy (STS), spatially resolved electronic information can be obtained. The potential of this method has been demonstrated for various cluster-support systems. A series of discrete STS resonances was detected for Pt clusters on HOPG, although a straightforward dependence on the cluster size could not be derived [7]. Quantization of surface states was observed on the top facet of Au and Ag clusters on HOPG [8–10]. Energy splitting and spatial localization of the levels could be rationalized by a two-dimensional (2D) particle-in-a-box model. On ligand stabilized metal particles, pronounced peaks in STS were ascribed to Coulomb charging effects caused by the localization of clusters between two tunnelling junctions [11,12].

In the present experiments, low-temperature STM and STS were employed to study the electronic properties of single Ag clusters deposited on $\text{Al}_2\text{O}_3/\text{NiAl}(110)$. Electron confinement in oxide supported metal clusters is believed to have a strong influence on their reactivity in heterogeneous catalysis [13,14]. Despite this importance for the understanding of catalytic processes, the electronic properties of single oxide-supported metal particles could not be determined so far. The ultra-thin Al_2O_3 film used in our experiments mimics essential properties of bulk alumina and efficiently decouples the cluster electron system from the underlying NiAl support [15]. Nonetheless, electron transport through the oxide remains possible and charging of the particles can be avoided. In contrast to earlier measurements on single metal particles [7–10], the spectral window for STS was largely extended in the present work and discrete energy levels resulting from electron confinement in the cluster volume could directly be observed.

The experiments were performed with an Eigler-type ultrahigh vacuum STM operated at 5 K. The

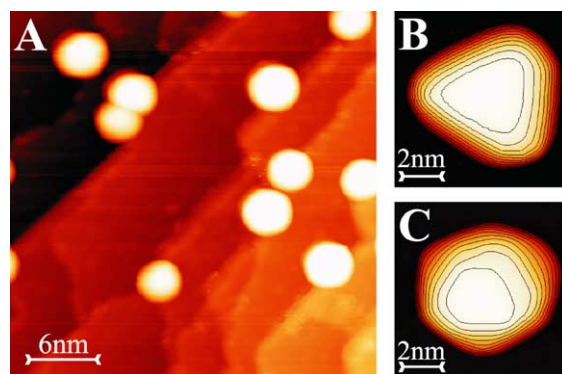


Fig. 1. (A) STM topographic image of Ag clusters on $\text{Al}_2\text{O}_3/\text{NiAl}(110)$ taken at $V_{\text{sample}} = 1.54 \text{ V}$, $I = 0.1 \text{ nA}$. Close up of a single cluster with (B) triangular and (C) hexagonal shape measured at $V_{\text{sample}} = -0.5 \text{ V}$, $I = 0.1 \text{ nA}$. Each contour line represents a height change of 0.4 nm.

$\text{NiAl}(110)$ surface was prepared by alternating sputter and anneal cycles followed by an exposure to 1200 L of O_2 at 580 K. Heating the crystal to 1100 K for 5 min resulted in the formation of a well-ordered Al_2O_3 film [15,16]. The quality of the film was controlled by LEED and STM measurements. The oxide consists of two Al–O layers and is approximately 0.5 nm in height. Its band gap of 8 eV is slightly smaller than in bulk alumina. Silver atoms were evaporated from a crucible and deposited at 400 K onto the oxide surface. Nucleation and growth of the clusters occur on oxide step edges, leading to the formation of isolated clusters with an average density of $5 \times 10^{11} \text{ cm}^{-2}$ (Fig. 1A). Cluster diameters could be adjusted between 5 and 12 nm by varying the Ag dose.¹ The particles preferentially grow with hemispherical shapes, but show sometimes well-defined triangular and hexagonal top facets (Fig. 1B and C). The geometry reflects the threefold symmetry of $\text{Ag}(111)$, indicating a crystalline structure and the presence of

¹ Cluster diameters were corrected to account for tip convolution effects, by comparing real amounts of deposited silver with amounts deduced from STM topographic images. The latter were obtained by summing up the apparent volume of Ag particles in representative STM images, using measured cluster heights, diameters and semi-ellipsoidal cluster shapes. The difference between apparent and real metal coverage provided a correction factor for the cluster diameters, which usually ranged between 1.5 and 2.

ordered (111) top facets [6]. The mean radius-to-height ratio of the clusters was determined to be 1.6. The cluster volume was taken to be the volume of a semi-ellipsoid with measured cluster height and diameter as input parameters.¹

The electronic properties of Ag particles on Al₂O₃/NiAl(110) were examined by conductance spectroscopy, detecting the first derivative of the tunnelling current as a function of sample bias (dI/dV) with a lock-in amplifier ($V_{\text{mod}} = 10\text{mV}$ rms). The dI/dV signal provides a measure of the local density of states (LDOS) in the cluster at the position of the tip. Fig. 2 shows a series of spectra taken in the centre of different Ag clusters in comparison to a spectrum of the bare Al₂O₃ film. The oxide conductance is characterized by a single broad maximum at -0.5V attributed to an electronic state localized at the NiAl–Al₂O₃ interface. The cluster spectra are dominated by a series of discrete dI/dV resonances, which are nearly equidistant in the examined energy range. Typical peak widths are as small as 50 mV. The peak positions are not symmetric with respect to the Fermi level and vary strongly from cluster to cluster. However, the energy separation ΔE between neighbouring peaks exhibits a distinct correlation with the cluster size. The level splitting in Fig. 2 decreases from 0.85 eV for the smallest cluster

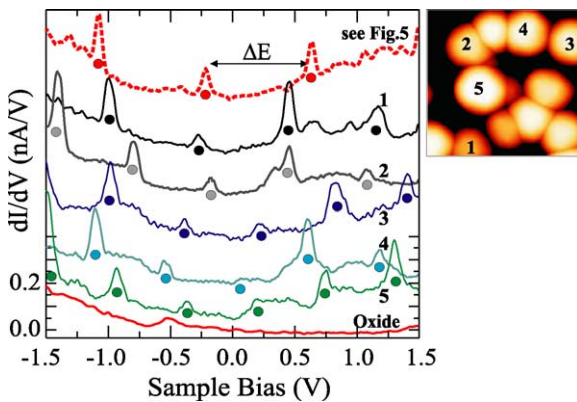


Fig. 2. (A) Conductance spectra of Ag particles on Al₂O₃/NiAl(110) and the bare oxide, taken at $V_{\text{sample}} = 1.5\text{V}$, $I = 1.0\text{nA}$. Equidistant dI/dV peaks in the clusters are marked by dots. The topmost spectrum refers to the set of dI/dV maps shown in Fig. 5. (B) Topographic STM image of the Ag clusters used for spectroscopy (image size: $50 \times 50\text{nm}^2$).

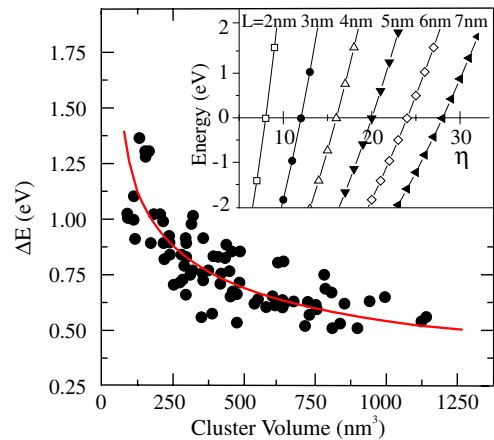


Fig. 3. Energy separation ΔE of measured dI/dV peaks versus cluster volume V for Ag particles on Al₂O₃/NiAl(110). The solid line is a least square fit of the data to $\Delta E \sim V^{-\alpha}$ with $\alpha \sim 0.3$. The inset shows calculated level energies for a particle-in-a-box with box lengths L comparable to real cluster heights.

($d = 7.5\text{nm}$) to 0.56 eV for the larger ones ($d = 12.5\text{nm}$). This trend of a decreasing peak-to-peak separation with increasing cluster size was generally observed for Ag clusters on Al₂O₃/NiAl(110) and is summarized in Fig. 3.

Information on the spatial localization of conductance peaks was obtained from series of dI/dV spectra taken along a line across the cluster surface. For the Ag particle shown in Fig. 4, five equidistant resonances P1–P5 have been identified. They shift to higher absolute energies and enlarge their mutual separation when moving the tip towards the cluster edge. The dispersion disappears for states close to the Fermi level and becomes larger with increasing distance from E_F . While the magnitude of spectral shifts is independent of the polarity, resonances above and below the Fermi level shift in opposite direction. The faint line between P4 and P5 shows no energy dispersion and is not equidistant to neighbouring levels. The respective dI/dV peak is most likely caused by the electronic structure of the tip. The cluster height for the tip positions in the spectral series has been added to Fig. 4.

The level shifts with increasing distance from the cluster centre were reproduced in dI/dV images, mapping the differential conductance over the cluster surface at a fixed bias value. Characteristic

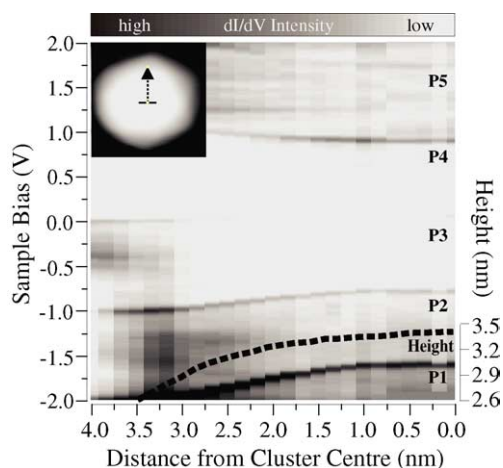


Fig. 4. Series of 25 dI/dV spectra taken along a line across a Ag cluster on $\text{Al}_2\text{O}_3/\text{NiAl}(110)$ ($V_{\text{sample}} = -1.5\text{ V}$, $I = 0.1\text{ nA}$). The spectra are plotted as a series of vertical lines, yielding a 2D representation of the energy levels as a function of position on the cluster surface. Tip positions are shown in the inset. Five dI/dV peaks P1–P5 can be identified, which shift to larger energies when the tip moves out of the cluster centre. The broken line indicates the cluster height at tip positions in the dI/dV series.

conductance maps for a Ag cluster on $\text{Al}_2\text{O}_3/\text{NiAl}(110)$ are shown in Fig. 5. The associated dI/dV spectrum taken in the cluster centre is presented in Fig. 2, uppermost curve. The dI/dV images are dominated by a ring of enhanced conductance, which originates from the resonance peak at -1.05 V in the dI/dV spectrum. The ring emerges in the cluster centre at this energy position and grows in diameter with increasing negative sample bias. When the ring diameter becomes comparable to the cluster size, it disappears from the dI/dV images. A similar ring system develops from the dI/dV resonance at -0.20 V and also expands for higher negative voltage. Rings originating from positive dI/dV peaks follow the opposite trend, i.e. they increase in diameter with increasing positive sample bias. The occurrence of rings of enhanced conductance directly reflects the hemispherical cluster shape, where distinct dI/dV resonances appear at the same energy on circles around the cluster centre. Obviously, the expansion of dI/dV rings with increasing sample bias is directly connected to shifts of the respective peak

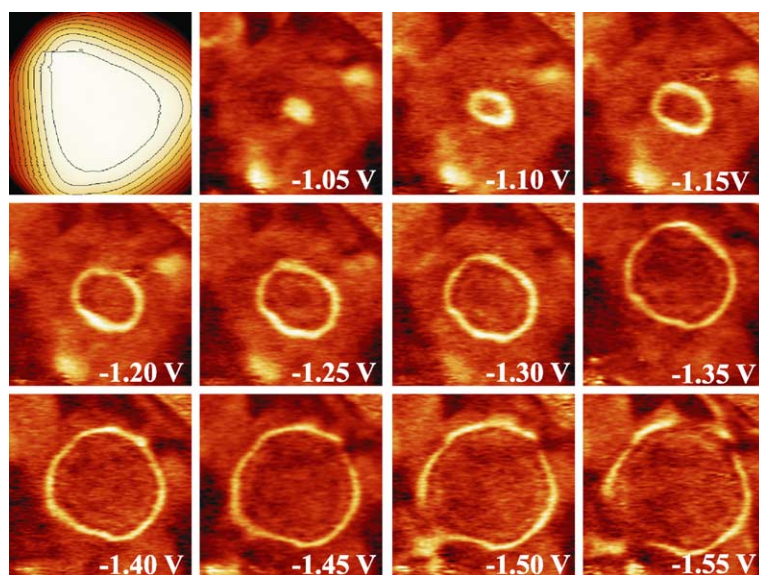


Fig. 5. Topographic (upper left panel) and dI/dV images of a Ag cluster on $\text{Al}_2\text{O}_3/\text{NiAl}(110)$ taken at the indicated sample bias (image size: $7.5 \times 7.5\text{ nm}^2$, $I = 0.1\text{ nA}$). Contour lines are separated by 0.4 nm . The corresponding dI/dV spectrum taken in the cluster centre is shown in Fig. 2, uppermost curve. The dI/dV maps exhibit a ring of enhanced conductance, which originates from the resonance at -1.05 V and expands for increasingly negative sample bias.

in spectra taken more and more outside the cluster centre.

The discussion of the results splits into two sections, (i) the presence of equidistant peaks in dI/dV spectra on oxide-supported Ag particles, and (ii) their spatial dispersion leading to rings of enhanced conductance. Equidistant dI/dV peaks have been earlier measured for metal particles located between two tunnelling junctions, the vacuum barrier and an insulating spacer between cluster and support [12,17]. Electron transport through a double barrier is hindered by the Coulomb repulsion between tunnelling electrons and residual charge on the centre electrode. Only electrons with an energy exceeding the Coulomb gap can overcome the barrier and contribute to the tunnelling current. Conductance spectra in the Coulomb regime are therefore determined by equidistant dI/dV peaks, whereby each step corresponds to an increase of the cluster charge by one elementary charge. Modelling the centre electrode as spherical capacitor, the Coulomb step width can be approximated by $\Delta V = e/(2\pi\epsilon_0\epsilon_r d)$ with d the cluster diameter and ϵ_r the dielectric constant of the environment ($\epsilon_r = 0.7\epsilon_{\text{vac}} + 0.3\epsilon_{\text{Al}_2\text{O}_3}$) [11,18]. For cluster sizes examined here, Coulomb gaps between 0.15 V ($d = 5$ nm) and 0.06 V ($d = 12$ nm) were calculated, ten times smaller than experimentally determined peak separations (Fig. 3). In addition, the 0.5 nm thick Al_2O_3 layer is relatively transparent for low energy electrons and charge transfer through the film occurs on a much shorter time scale than consecutive tunnelling events. An effective charging of Ag particles inducing Coulomb behaviour can therefore be excluded as possible interpretation for the observed dI/dV spectra.

More likely, the conductance spectra reflect the intrinsic LDOS of Ag particles affected by the quantization of electronic states in the spatially confined system [19]. Quantized surface states have been observed on the top facet of Ag and Au particles on HOPG using STS [8–10]. These resonances start at an energy close to the onset of the unconfined surface band (-65 mV for Ag(111)) and are not equidistant in energy. The observation of peaks with constant energy separation over a much wider bias range prohibits a similar interpre-

tation for the present data. Approximately equidistant LDOS levels have been detected by photoelectron spectroscopy and STS for Ag films on GaAs and HOPG [20,21] and Pb films on Cu(111) [22,23]. The level separation showed a decrease with increasing film thickness, which was attributed to a quantization of electronic states perpendicular to the film surface. Peak separations measured for Ag particles on $\text{Al}_2\text{O}_3/\text{NiAl}(110)$ cover a similar range and would also be consistent with quantization effects along the particle height. In such a case, the discretization would be truly one-dimensional and electron confinement in planes parallel to the cluster-oxide interface would be of minor importance. In a simple particle-in-a-box model, peak separations scale with the dimensionality of the confined system $\Delta E \sim V^{-\alpha}$ [24]. For quantization in a 3D system the scaling factor α is 1, it becomes 2/3 in 2D and 1/3 in a 1D system. Fitting the correlation between experimental peak separation and cluster volume yields a scaling factor α of roughly 0.3, suggesting a discretization of electronic states along the cluster height. A 1D particle-in-a-box model also provides a crude estimation of the expected energy gaps between the levels. Electronic states in a 1D quantum well with infinite walls are given by [24]: $E_n = E_0 + \frac{\hbar^2}{2m_e} \left(\frac{n\pi}{L}\right)^2$. To approach the experimental situation, typical cluster heights were chosen for the well length L and E_0 was taken to match the onset of the bulk Ag *sp* band at -5.5 eV (Fig. 3 inset) [25]. For states with high quantum numbers n , the parabolic dispersion is nearly washed out and peaks appear to be equidistant close to the Fermi level, as observed in the experiment (Fig. 3 inset). Furthermore, calculated peak-to-peak separations cover the same energy range as the experimental splittings. However, the simplicity of the model prohibits any quantitative description of the electron confinement in the cluster, as it neglects the finite depth of the potential, phase shifts at the cluster-vacuum and cluster-oxide interfaces and the curvature of the cluster top facet.

Assuming a preferential growth of particles with [111] orientation, a level quantization along the cluster height would mostly affect the electron band in Γ - L direction of the Brillouin zone, which has a pronounced gap between -0.3 and 4.0 eV in

bulk silver [19,25]. In the present experiment on Ag particles, the energy levels cross the Fermi level without evidence of this gap. The suppression of the forbidden zone for electronic states is rather unexpected for particles of this size and could be an indication for a growth direction different from Ag[111], where bulk bands show no gap at the Fermi level.

Spatial confinement in planes parallel to the surface should also lead to a quantization of electronic states. The level splitting would scale with the inverse area of the 2D planes and is expected to be much smaller than along the cluster height. On the flat top facets of Au particles on HOPG, a quantized surface state has indeed been identified by STS [9,10]. For Ag particles on the Al_2O_3 film, a corresponding dI/dV signature was not detected, which might be due the strongly curved cluster surface, but also due to a growth direction deviating from Ag[111].

Spatially resolved dI/dV spectra of Ag particles revealed a shift of the LDOS resonances to higher energies and an increase of their mutual separation, when moving the tip away from the cluster centre. This observation would be in principle consistent with an enhanced electron quantization at positions of reduced cluster height (see inset of Fig. 3) [24]. However, several arguments are in conflict with such an interpretation. The examined particles have sizes in the range of the Ag Fermi wavelength and represent quantum-mechanical units with constant level energies throughout their diameter [23]. The observed shifts have opposite signs for peaks at positive and negative sample bias and disappear for states at the Fermi level. Using the picture of a position-dependent electron quantization in the cluster, the reversed dispersion of electronic states requires a switching from electron- to hole-like effective masses at the Fermi level. Such an assumption is not justified by experimental evidence and could not be observed in comparable systems before. More severely, the observed level dispersion should depend on the cluster size with larger shifts occurring in smaller particles due to the lower quantum numbers involved. However, no unambiguous dependence of the level shifts on the cluster volume could be derived from the experimental data.

A plausible explanation for the observed behaviour can be found by considering the influence of the tip-induced electric field on the cluster electronic system. In conductance spectra taken with disabled feedback loop, the tip electric field directly scales with the sample bias. Resonances at higher energies are affected by stronger fields and show larger shifts compared to states at the Fermi level. Furthermore, states at positive and negative polarity feel reverse field directions and disperse in opposite manner, as observed in the experiment. The spatial shift of level energies can be understood in terms of a decreasing tip-oxide distance when moving from the centre to outer parts of the Ag particles. Above the cluster centre, the tip-oxide distance is maximal and the tip electric field is efficiently screened at the Ag surface. The applied sample bias entirely drops in the vacuum barrier between tip and cluster and the effective cluster potential is only weakly affected by the presence of the tip (Fig. 6A). As the tip moves down the cluster, the influence of the electric field on the Al_2O_3 support increases. The small screening efficiency of the oxide surface leads to a considerable penetration of the field and initiates a band bending in direction of the field gradient [26]. A fraction of the sample bias now drops inside the oxide film, reducing the apparent potential at the cluster surface (Fig. 6B). An electronic state, which was detected at a voltage V_0 in the cluster centre, cannot be reached at the cluster edge. An additional voltage ΔV has to be applied to compensate

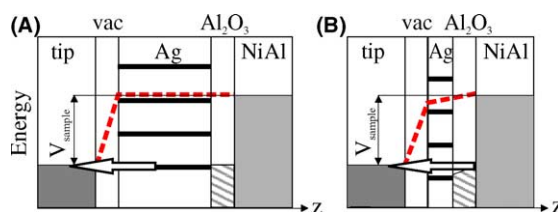


Fig. 6. Potential diagram for a tunnelling junction containing tip, vacuum barrier, Ag cluster, Al_2O_3 film and NiAl support. (A) sketches tunnelling into the cluster centre and (B) into its outer parts. The broken line indicates the electron potential across the tunnelling junction. Whereas the sample bias completely drops in the vacuum barrier in (A), it partly penetrates into the oxide film in (B). Energy levels of the cluster in (B) are therefore detected at a higher sample bias than in (A).

for the voltage drop in the oxide film and the cluster resonance is measured at higher absolute energies. This shift of the resonance condition with decreasing cluster height in combination with the radial cluster symmetry leads to the occurrence of rings of enhanced conductance, which expand on the cluster surface with increasing sample bias.

Tip-induced shifts of the cluster levels should exclusively depend on the tip-oxide distance.² A correlation between level dispersion and tip height was indeed observed in spectral series taken on the Ag particles (Fig. 5). However, the tip height is not the only factor controlling the peak shifts and rings of enhanced conductance do not perfectly correspond to contour lines of the cluster height. This discrepancy is most likely caused by the non-local character of the tip-induced electric field, which influences the cluster potential in a wide area. Especially for relatively blunt tips and clusters with close neighbours, the spatial pattern induced by the LDOS peaks can be distorted to almost arbitrarily shapes on the cluster surface.

The maximum bending of the oxide bands and the corresponding peak shifts depend on the static dielectric constant ϵ_r of the Al_2O_3 layer. Taking the bulk ϵ_r of approximately 10 and a similar thickness for vacuum gap and oxide film (0.5 nm), 10% of the applied voltage drops in the Al_2O_3 layer [18]. For a peak position at -1.5 V, the maximum shift would be in the order of -0.15 V, which agrees well with experimental values. As the dielectric properties of the ultra-thin Al_2O_3 layer might be different from the bulk material, real shifts of the LDOS levels could be even larger.

In conclusion, STS experiments on individual Ag particles on $\text{Al}_2\text{O}_3/\text{NiAl}(110)$ revealed a series of discrete electron levels, separated by gaps between 1.0 and 0.5 eV for particles containing between 5,000 and 50,000 atoms, respectively. The occurrence of discrete energy levels was explained

by an electron confinement along the particle height. This assignment has certainly speculative character and needs to be confirmed by a more sophisticated model. However, the observed size dependence of electronic properties in Ag clusters demonstrates the importance of quantum effects even in medium-sized metal particles.

Acknowledgment

We are grateful to K. Horn for stimulating discussions. M.K. thanks the 'Studienstiftung des deutschen Volkes' for support.

References

- [1] B.C. Gates, L. Guzzi, H. Knoezinger (Eds.), *Metal Cluster in Catalysis*, Elsevier, Amsterdam, 1986.
- [2] G. Schmid (Ed.), *Clusters and Colloids: From Theory to Applications*, VCH, Weinheim, 1994.
- [3] U. Kreibitz, M. Vollmer, *Optical Properties of Metal Clusters*, Springer, Berlin, 1995.
- [4] Y.Q. Cai, A.M. Bradshaw, Q. Guo, D.W. Goodman, *Surf. Sci.* 399 (1998) L357.
- [5] H. Hövel, B. Grimm, M. Pollmann, B. Reihl, *Phys. Rev. Lett.* 81 (1998) 4608.
- [6] K. Højrup Hansen, T. Worren, S. Stempel, E. Laegsgaard, M. Baeumer, H.-J. Freund, F. Besenbacher, I. Stensgaard, *Phys. Rev. Lett.* 83 (1999) 4120.
- [7] A. Bettac, L. Köller, V. Rank, K.H. Meiwes-Broer, *Surf. Sci.* 402 (1998) 475.
- [8] H. Hövel, B. Grimm, M. Bödecker, K. Fieger, B. Reihl, *Surf. Sci.* 463 (2000) L603.
- [9] I. Barke, H. Hövel, *Phys. Rev. Lett.* 90 (2003) 166801.
- [10] H. Hövel, I. Barke, *New J. Phys.* 5 (2003) 31.
- [11] A. Hanna, M. Tinkham, *Phys. Rev. B* 44 (1991) 5919.
- [12] J. Hou, B. Wang, J. Yang, X. Wang, H.Q. Wang, Q. Zhu, X. Xiao, *Phys. Rev. Lett.* 86 (2001) 5321.
- [13] M. Valden, X. Lai, D.W. Goodman, *Science* 281 (1998) 1647.
- [14] U. Heiz, A. Sanchez, S. Abbet, W.-D. Schneider, *J. Am. Chem. Soc.* 121 (1999) 3214.
- [15] M. Bäumer, H.-J. Freund, *Prog. Surf. Sci.* 61 (1997) 7.
- [16] G. Ceballos, Z. Song, J.I. Pascual, H.-P. Rust, H. Conrad, M. Baeumer, H.-J. Freund, *Chem. Phys. Lett.* 359 (2002) 41.
- [17] M. Kulawik, N. Nilius, H.-P. Rust, H.-J. Freund, *Phys. Rev. Lett.* 91 (2003) 256101.
- [18] H. Osman, J. Schmidt, K. Svensson, R.E. Palmer, Y. Shigeta, J.P. Wilcoxon, *Chem. Phys. Lett.* 330 (2000) 1.
- [19] J. Fontanella, C. Andeen, D. Schuele, *J. Appl. Phys.* 45 (1974) 2852.

² Strong variations in the set-point conditions for dI/dV spectroscopy also induce small shifts of the energy levels in Ag clusters. The levels are detected at smaller absolute energies for larger set-point voltages and lower tunnelling currents, due to the increased tip-oxide distance and the reduced band bending.

- [19] T.C. Chiang, Surf. Sci. Rep. 39 (2000) 181.
- [20] D.A. Evans, M. Alonso, R. Cimino, K. Horn, Phys. Rev. Lett. 70 (1993) 3483.
- [21] F. Patthey, W.-D. Schneider, Phys. Rev. B 50 (1994) 17560.
- [22] I.B. Altfeder, K.A. Matveev, D.M. Chen, Phys. Rev. Lett. 78 (1997) 2815.
- [23] R. Otero, A.L. Vazquez de Parga, R. Miranda, Phys. Rev. B 66 (2002) 115401.
- [24] C. Kittel, Introduction to Solid State Physics, Wiley, New York, 1996.
- [25] D.A. Papaconstantopoulos, Handbook of Band Structures of Elemental Solids, Plenum Press, New York, 1986.
- [26] D.A. Bonnell, J. Am. Ceram. Soc. 81 (1998) 3049.